Korean J. Chem. Eng., 34(12), 3067-3076 (2017)
DOI: 10.1007/s11814-017-0219-6

pISSN: 0256-1115
eISSN: 1975-7220

Constraint handling optimal PI control of open-loop unstable process: Analytical approach

Rodrigue Tchamna and Moonyong Lee†

School of Chemical Engineering, Yeungnam University, Gyeongsan 38541, Korea
(*Received 19 April 2017 • accepted 9 August 2017*)

Abstract−This paper proposes the closed-form analytical design of proportional-integral (PI) controller parameters for the optimal control of an open-loop unstable first order process subject to operational constraints. The main idea of the design process is not only to minimize the control performance index, but also to cope with the constraints in the process variable, controller output, and its rate of change. To derive an analytical design formula, the constrained optimal control problem in the time domain was transformed to an unconstrained optimization in a parameter space associated with closed-loop dynamics. By taking advantage of the proposed analytical approach, a convenient shortcut algorithm was also provided for finding the optimal PI parameters quickly, based on the graphical analysis for the optimal solution of the corresponding optimization problem in the parameter space. The resulting optimal PI controller guarantees the globally optimal closed-loop response and handles the operational constraints precisely.

Keywords: Optimal Control, Operational Constraints, Open-loop Unstable Process, Industrial Proportional-Integral (PI) Controller, Analytical Design Approach

INTRODUCTION

Optimal control of open-loop unstable processes is usually more demanding and laborious than that of stable systems. This is due mainly to the unstable nature of the dynamics, for which most conventional design techniques fail. For example, techniques such as the well-known Ziegler and Nichols achieve satisfactory performance for the control of stable systems, but cannot be applied directly to unstable systems. On the other hand, optimal servo control plays a major role and has a direct effect on the safety and performance of many industrial chemical processes. Typical examples of such systems include chemical reactors [1], absorption towers using swirling gas flow [2], and level control systems [3]. Among many other control products, pneumatic robot systems also rely mainly on accurate servo control [4], as well as vibration isolation systems [5]. Two factors, the challenge in controlling unstable systems and the importance of servo systems in process industries, motivate this study of the optimal servo control of unstable systems under operational constraints.

Considerable research has been done to control unstable processes. Huang and Chen suggested an auto-tuning procedure for PID controllers for a more general class of unstable processes [6]. Jung et al. presented a direct synthesis tuning method for the PI controller settings of unstable first-order-plus-time-delay processes [7]. Jacob and Chidambaram designed an explicit design formula for feedback controllers using a model reference, synthesis method and internal model control for an unstable first-order plus time delay system [8]. On the other hand, to the best of the authors' knowledge, there has been no research on the analytical optimal servo control of unstable processes subject to operational constraints. The objective of constrained optimal control is to minimize the control cost subject to constraints. Generally, typical operational constraints include the actuator magnitude and its rate saturation, process/output variable, and internal state variables. Constraints are inherent in any industrial control system, either implicitly or explicitly. These constraints are generally associated with both the process variable and controller output. A well designed optimal control would fail in a real life situation if the constraints were not taken into account at the controller design stage. To avoid trial and error and reduce the design effort, these operational constraints should be considered and handled in the design process, not after the fact. Some techniques that deal with the constraints in control systems include anti-windup and bumpless transfer (AWBT) [9] and constrained model predictive control [10]. The AWBT approach suggests a way to overcome the problem of windup, which occurs when an unstable controller is subject to input saturation [9]. This method is good because it can be added to any existing unconstrained linear controller. However, the problem is that stability is not guaranteed [11]. As for the constrained model predictive control, the method is the most popular when it comes to constrained optimization, but the computational cost of the on-line optimization process is its main drawback due to the numerical optimization between two sample times. Moreover, this approach is a black box approach and the relationship between the control and process parameters is not explicit. To overcome this issue, an analytical solution of an optimal PI controller under constraint was proposed previously for a regulatory problem [12-14], and a servo problem [15] of an integrating process. The work was extended to a stable system [16].

This paper makes a new contribution by developing the analyti-

†To whom correspondence should be addressed.
E-mail: mynlee@yu.ac.kr

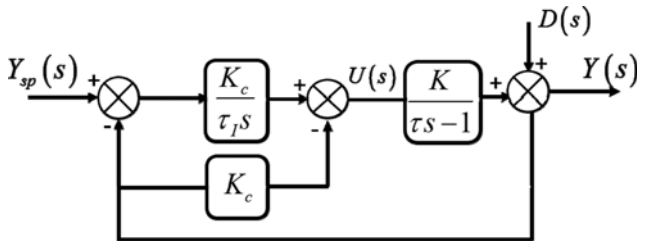

Fig. 1. Feedback control block diagram of the first order unstable process.

cal design for the optimal servo controller handling the operation constraints for open-loop unstable process. For this, the optimal control formulation subject to constraints was first transformed to an equivalent unconstrained optimization in new parameter space by applying the Lagrange multiplier with an astute parameterization. The optimal PI tuning rules were then derived based on a thorough graphical examination of the possible location of the global optimum in newly introduced parameter space. Simulation was carried out for a typical first-order open-loop unstable process, and the effects of the weighting factors and process parameters were discussed.

METHODOLOGY AND DESIGN

1. Formulation of Constrained Optimal Control

Fig. 1 presents a schematic diagram of the open-loop unstable process considered in this work. It is a type-C PI controller, also called I-P controller, which is a modified type of PID controller where the set point is removed from the proportional term in order to avoid the initial quick on the manipulated variable for a step change in the set point. The major resulting transfer functions from this figure are as follows:

$$\mathrm{Y(s)}=\frac{1}{\varepsilon\tau_c\tau_I s^2+\varepsilon\tau_I s+1}\mathrm{Y}_{sp}(s) \tag{1}$$

$$\mathrm{U(s)}=\frac{\frac{1}{\mathrm{K}}(s\tau-1)}{\varepsilon\tau_c\tau_I s^2+\varepsilon\tau_I s+1}\mathrm{Y}_{sp}(s) \tag{2}$$

where

$$\tau_c=\frac{\tau}{\mathrm{KK}_c-1}=\frac{\tau}{\varepsilon\mathrm{KK}_c} \tag{3-1}$$

$$\varepsilon=\frac{\tau}{\tau+\tau_c} \tag{3-2}$$

Let ζ be the damping ratio of the system above. It can be expressed as follows:

$$\zeta=\frac{1}{2}\sqrt{\frac{\varepsilon\tau_I}{\tau_c}}=\frac{1}{2}\sqrt{\frac{\tau}{\tau+\tau_c}\frac{\tau_I}{\tau_c}} \tag{3-3}$$

The performance index of the system consists of the weighted sum of the process variable error, e(t), along with the rate of controller output change, u′(t), which is to be minimized. The system is subject to a step change, ΔY_{sp}, in a set-point or output disturbance. The constraints to be satisfied are (1) maximum permissible value of the process variable, i.e., y_{max}; (2) maximum permissible value of the controller output, i.e., u_{max}; and (3) maximum permissible value of the rate of the controller output change, u'_{max}. Consequently, the constrained optimal formulation boils down to deriving the parameters of the controller for which the performance index in Eq. (4-1) is minimized for a step change in input ΔY_{sp}/s

$$\min \Phi=\omega_y\int_0^\infty(\mathrm{e(t)})^2\mathrm{dt}+\omega_{u'}\int_0^\infty(\mathrm{u'(t)})^2\mathrm{dt} \tag{4-1}$$

and satisfying the constraints

$$|\mathrm{y(t)}|\le \mathrm{y}_{max} \tag{4-2}$$

$$|\mathrm{u'(t)}|\le \mathrm{u}'_{max} \tag{4-3}$$

$$|\mathrm{u(t)}|\le \mathrm{u}_{max} \tag{4-4}$$

where

$$\mathrm{e(t)}=\mathrm{y}_{sp}(\mathrm{t})-\mathrm{y(t)} \tag{4-5}$$

Deriving an analytical solution for the optimal PI parameters directly from the constrained non-linear optimization above is virtually impossible. Moreover, no numerical optimization approach guarantees a global optimal solution. To address this limitation, a clever parameterization was introduced through which the constrained optimal control problem above could be transformed to a simple algebraic form to provide an analytical form of solution and allow graphical analysis for the optimal control problem. The constrained optimal control problem in Eqs. (4-1) to (4-4) was transformed algebraically based on two variables, τ_c and ζ, as follows (See Appendix for derivation details):

$$\min \Phi(\tau_c,\,\zeta)=\alpha\tau_c(4\zeta^2+1)+\frac{\beta(4\tau_c^2\zeta^2+\tau^2)}{\tau^2\tau_c^3\zeta^4} \tag{5-1}$$

subject to

$$\gamma_g\ge \mathrm{g}(\zeta) \tag{5-2}$$

$$\tau_c^2\gamma_h\ge \mathrm{h}(\zeta) \tag{5-3}$$

$$\gamma_f\ge \mathrm{f}(\zeta,\,\tau_c) \tag{5-4}$$

where

$$\alpha=\frac{\omega_y\Delta\mathrm{Y}_{sp}^2}{2};\ \beta=\frac{\omega_{u'}}{32}\left(\frac{\tau\Delta\mathrm{Y}_{sp}}{\mathrm{K}}\right)^2;\ \gamma_g=\left|\frac{\mathrm{y}_{max}}{\Delta\mathrm{Y}_{sp}}\right|;\ \gamma_f=\left|\frac{\mathrm{K}}{\Delta\mathrm{Y}_{sp}}\mathrm{u}_{max}\right|;\ \gamma_h=\left|\frac{\mathrm{K}}{\tau}\frac{\mathrm{u}'_{max}}{\Delta\mathrm{Y}_{sp}}\right| \tag{6}$$

See Eqs. (A14), (A20), and (A24) in the Appendix for the expressions of g(ζ), f(ζ), and h(ζ). Note that all three constraints in the above equations are now expressed as a function of τ_c and ζ. This indicates that the conditions and characteristics of optimal solution can be examined by graphical observations for the contour of the objective function and the functions associated with the three constraints in (ζ, τ_c) space.

2. Classification of Global Optimum for Controller Design

Applying the Lagrangian multiplier [17] converts to the constrained problem posed in Eqs. (5-1) to (5-4) to the following unconstrained equivalent problem:

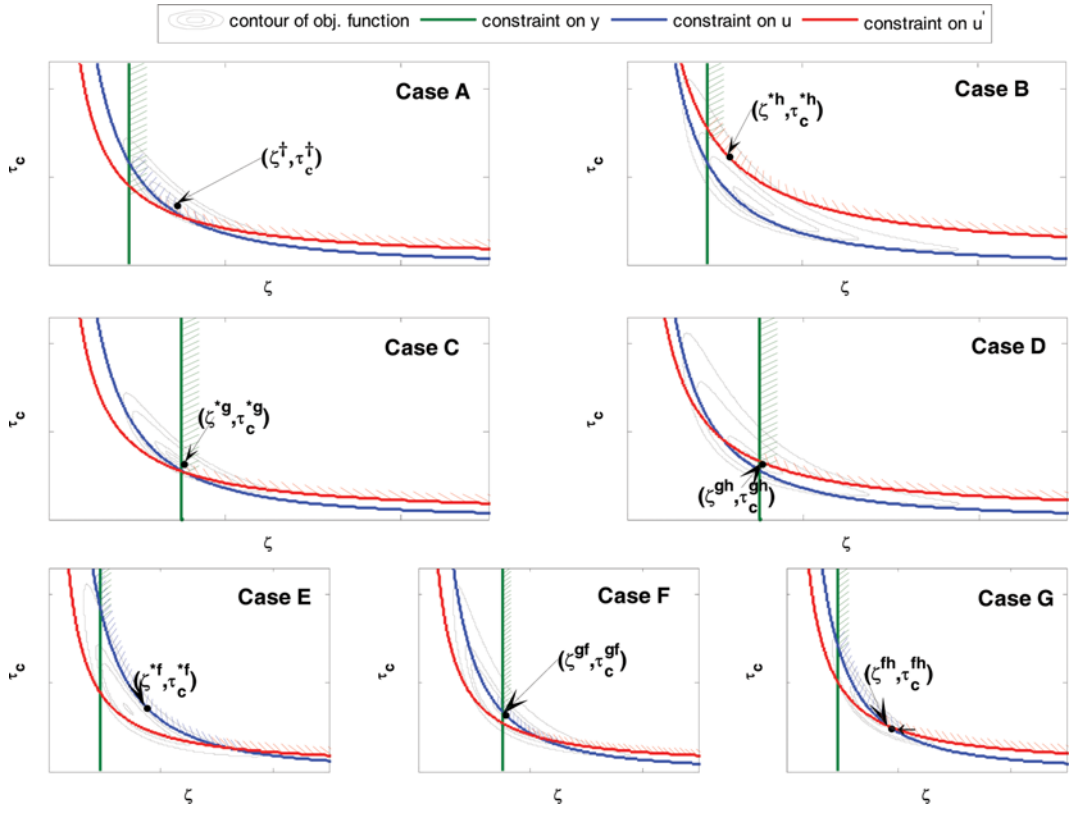

Fig. 2. Contours, constraints and possible locations of the global optimum.

$$\begin{aligned}\min L(\tau_c, \zeta, \varpi_1, \varpi_2, \varpi_3, \sigma_1, \sigma_2, \sigma_3) &= \alpha\tau_c(4\zeta^2+1) \\ &+ \frac{\beta(4\tau_c^2\zeta^2+\tau^2)}{\tau^2\tau_c^3\zeta^4} + \varpi_1(\tau_c^2\gamma_h - h(\zeta) - \sigma_1^2) \\ &+ \varpi_2(\gamma_g - g(\zeta) - \sigma_2^2) + \varpi_3(\gamma_f - f(\zeta, \tau_c) - \sigma_3^2)\end{aligned} \tag{7}$$

where, σ_i is the slack variable and ϖ_i ($\varpi_i \le 0$) the Lagrange multiplier. The solution is only the optimum if the following conditions are satisfied:

$$\frac{\partial L}{\partial \tau_c} = \frac{\partial \phi}{\partial \tau_c} + \varpi_1(2\tau_c\gamma_h) + \varpi_3\left[-\frac{\partial f(\zeta, \tau_c)}{\partial \tau_c}\right] = 0 \tag{8}$$

$$\frac{\partial L}{\partial \zeta} = \frac{\partial \phi}{\partial \zeta} - \varpi_1\left(\frac{\partial h(\zeta)}{\partial \zeta}\right) - \varpi_2\frac{\partial g(\zeta)}{\partial \zeta} - \varpi_3\frac{\partial f(\zeta, \tau_c)}{\partial \zeta} = 0 \tag{9}$$

$$\frac{\partial L}{\partial \varpi_1} = \tau_c^2\gamma_h - h(\zeta) - \sigma_1^2 = 0 \tag{10}$$

$$\frac{\partial L}{\partial \varpi_2} = \gamma_g - g(\zeta) - \sigma_2^2 = 0 \tag{11}$$

$$\frac{\partial L}{\partial \varpi_3} = \gamma_f - f(\zeta, \tau_c) - \sigma_3^2 = 0 \tag{12}$$

$$\begin{aligned}&\frac{\partial L}{\partial \sigma_i} = -2\varpi_1\sigma_1 = 0; \\ &\frac{\partial L}{\partial \sigma_2} = -2\varpi_2\sigma_2 = 0;\ \frac{\partial L}{\partial \sigma_3} = -2\varpi_3\sigma_3 = 0\end{aligned} \tag{13}$$

The seven optimal cases were obtained by solving Eqs. (8) to (13) for the corresponding combination of slack variables $\sigma_i \neq 0$ and the Lagrange multiplier, $\varpi_i = 0$, $\varpi_i \neq 0$. Fig. 2 illustrates the seven possible locations of the global optimum for the optimization problem, which can be: 1) inside the feasible region (case A), 2) on one of the constraints (cases B, C, or E), or 3) on the intersection of two constraints (cases D, F, or G).

Note that Karush-Kuhn-Tucker (KKT) condition [18] can also be applied to derive the analytical relations associated with the optimal control. The only difference between the Lagrangian multiplier method and the KKT method is in the equality or inequality constraint. In fact, rigorously speaking, the Lagrangian multiplier deals with equalities constraints, while the KKT deals with both equalities and inequalities constraints. Converting inequality constraints to equality constraints results in the Lagrangian multiplier method.

Table 1 summarizes the conditions that lead to each global optimal location. The derivation of these conditions is possible from the visual examination of the shape and trend of the above contours and constraints.

Case A: The extreme point, $(\zeta^{\dagger}, \tau_c^{\dagger})$, is the global optimum because it is located inside the feasible region.

Case B: The global optimum, $(\zeta^{*h}, \tau_c^{*h})$, is located on the constraint, $\tau_c^2\gamma_h - h(\zeta) = 0$.

Case C: The global optimum, $(\zeta^{*g}, \tau_c^{*g})$, is on the constraint $g(\zeta) = \gamma_g$. Because $g(\zeta)$ is only a function of the damping ratio ζ, ζ^{*g} as the solution of equation $g(\zeta) = \gamma_g$ is also a constant value and equivalent to the minimum allowable damping factor of the system, γ_{min}.

Case D: The global optimum, $(\zeta^{gh}, \tau_c^{gh})$, is located on the ver-

Table 1. Global optima of the constrained optimization problem in Eqs. (5-1) to (5-4)

Case	Constraint specification	Condition	Global optimum	Location of global optimum	Calculation of global optimum
A	mild u'_{max} mild y_{max} mild u_{max}	$\zeta_{min} \le \zeta^{\dagger}$ and $\tau_c^{\dagger} \ge \max(\tau_c^{*h}, \tau_c^{*f})$	$(\zeta^{\dagger}, \tau_c^{\dagger})$	In the interior of the feasible region.	$\zeta^{\dagger} = \left[\frac{1}{2} + \frac{1}{\tau^2}\left(\frac{\beta}{\alpha}\right)^{1/2}\right]^{1/2}$; $\tau_c^{\dagger} = \frac{1}{\zeta^{\dagger}}\left(\frac{\beta}{\alpha}\right)^{1/4}$
B	tight u'_{max} mild y_{max} mild u_{max}	$\zeta^{*h} > \max(\zeta^{hf}, \zeta_{min})$ and $\tau_c^{\dagger} < \max(\tau_c^{*h}, \tau_c^{*f})$	$(\zeta^{*h}, \tau_c^{*h})$	on $\tau_c^2 = \gamma_h^{-1} h(\zeta)$	$\zeta^{*h} = \left(\frac{4\beta\gamma_h^2}{\alpha} + \frac{4\beta\gamma_h}{\alpha\tau^2} + \frac{1}{4}\right)^{1/2}$ $\tau_c^{*h} = (\gamma_h^{-1} h(\zeta^{*h}))^{1/2}$
C	mild u'_{max} tight y_{max} mild u_{max}	$\zeta_{min} > \zeta^{\dagger}$ and $\tau_c^{*g} > \max(\tau_c^{gh}, \tau_c^{gf})$	$(\zeta^{*g}, \tau_c^{*g})$	on $g(\zeta) = \gamma_g$	$g(\zeta^{*g}) = \gamma_g$ $\tau_c^{*g} = \left(\frac{2\beta + \sqrt{12\tau^4\alpha\beta\zeta^2 + 3\tau^4\alpha\beta + 4\beta^2}}{\tau^2\alpha(4\zeta^2+1)\zeta^2}\right)^{1/2}\Big\|_{\zeta=\zeta^{*g}}$
D	tight u'_{max} tight y_{max} mild u_{max}	$[\tau_c^{\dagger} \ge \max(\tau_c^{*h}, \tau_c^{*f})$ and $\zeta_{min} > \zeta^{\dagger}$ and $\tau_c^{gh} > \max(\tau_c^{*g}, \tau_c^{gf})]$ or $[\tau_c^{\dagger} < \max(\tau_c^{*h}, \tau_c^{*f})$ and $\zeta^{gh} > \max(\zeta^{hf}, \zeta^{*h})]$	$(\zeta^{gh}, \tau_c^{gh})$	on the vertex by $g(\zeta) = \gamma_g$ and $\tau_c^2 = \gamma_h^{-1} h(\zeta)$	$g(\zeta^{gh}) = \gamma_g$ $\tau_c^{gh} = (\gamma_h^{-1} h(\zeta^{gh}))^{1/2}$
E	mild u'_{max} mild y_{max} tight u_{max}	$\tau_c^{\dagger} < \max(\tau_c^{*h}, \tau_c^{*f})$ and $\zeta_{min} < \zeta^{*f} < \zeta^{hf}$	$(\zeta^{*f}, \tau_c^{*f})$	on $f(\zeta, \tau_c) = \gamma_f$	$\begin{cases} \gamma_f = f(\zeta^{*f}, \tau_c^{*f}) \\ \frac{\partial f(\zeta,\tau_c)}{\partial \tau_c}\frac{\partial \phi}{\partial \zeta} - \frac{\partial f(\zeta,\tau_c)}{\partial \zeta}\frac{\partial \phi}{\partial \tau_c} = 0 \end{cases}$
F	mild u'_{max} tight y_{max} tight u_{max}	$[\tau_c^{\dagger} \ge \max(\tau_c^{*h}, \tau_c^{*f})$ and $\zeta_{min} > \zeta^{\dagger}$ and $\tau_c^{gf} > \max(\tau_c^{*g}, \tau_c^{gh})]$ or $[\tau_c^{\dagger} < \max(\tau_c^{h}, \tau_c^{*f})$ and $\zeta^{*f} < \zeta_{min} < \zeta^{hf}]$	$(\zeta^{gf}, \tau_c^{gf})$	on the vertex by $f(\zeta, \tau_c) = \gamma_f$ and $g(\zeta) = \gamma_g$	$\begin{cases} g(\zeta^{gf}) = \gamma_g \\ \gamma_f = f(\zeta^{gf}, \tau_c^{gf}) \end{cases}$
G	tight u'_{max} mild y_{max} tight u_{max}	$\tau_c^{\dagger} < \max(\tau_c^{*h}, \tau_c^{*f})$ and $\zeta_{min} < \zeta^{*h} < \zeta^{hf}$	$(\zeta^{fh}, \tau_c^{fh})$	on the vertex by $f(\zeta, \tau_c) = \gamma_f$ and $\tau_c^2 = \gamma_h^{-1} h(\zeta)$	$\gamma_f = f(\zeta^{hf}, \tau_c^{hf})$ $\tau_c^{hf} = \frac{1}{2\zeta^{hf}\sqrt{\gamma_h}}$

tex point formed by $\tau_c^2\gamma_h - h(\zeta)=0$ and $g(\zeta)=\gamma_g$. Here, ζ^{gh} is also equivalent to ζ_{min}.

Case E: The global optimum, $(\zeta^{*f}, \tau_c^{*f})$, is located on $\gamma_f - f(\zeta, \tau_c) = 0$.

Case F: The global optimum, $(\zeta^{gf}, \tau_c^{gf})$, is located on the vertex point formed by $\gamma_f - f(\zeta, \tau_c)=0$ and $g(\zeta)=\gamma_g$.

Case G: The global optimum, $(\zeta^{hf}, \tau_c^{hf})$, is on the vertex point formed by $\gamma_f - f(\zeta, \tau_c)=0$ and $\tau_c^2\gamma_h - h(\zeta)=0$.

After obtaining the global optimum for a particular case, the optimal parameters of the PI controller can be found in a straightforward manner using Eqs. (3-1) and (3-2), as follows:

$$K_c = \frac{\tau}{K}\frac{\varepsilon^{opt}}{\tau_c^{opt}};\ \tau_I = 4(\zeta^{opt})^2\frac{\tau_c^{opt}}{\varepsilon^{opt}} \tag{14-1}$$

where

$$\varepsilon^{opt} = \frac{1}{\left(1 + \frac{\tau_c^{opt}}{\tau}\right)} \tag{14-2}$$

3. Determination of Feasible Region

The optimal solution summarized in Table 1 is only true if the constraints set is such that a solution exists. Indeed, depending on the constraint set, the optimal solution may not have a feasible solution. Therefore, before applying the constrained optimal control formulation, any given constraint set should first be screened quickly to determine its basic feasibility. From Eqs. (A11), (A17), and (A22) in the Appendix, it can be shown that for the constraints by y_{max} and u_{max} to be feasible, they must be greater than $|\Delta Y_{sp}|$ and $|\Delta Y_{sp}/K|$, respectively, whereas the constraint by u'_{max} can be set to any non-negative value. Fig. 3 illustrates how the three constraints specifications affect the feasible region. The constraint $\gamma_g \ge g(\zeta)$ vertically splits the region into two, while the constraints imposed by $\tau_c^2\gamma_h \ge h(\zeta)$ and $\gamma_f \ge f(\zeta, \tau_c)$ have a similar shape in (ζ, τ_c) space.

Fig. 3 shows that for any feasible constraint set, y_{max}, u_{max}, and u'_{max}, the feasible region is bounded below but unbounded in the upper side. This means that a decrease in y_{max}, u_{max}, and u'_{max} will narrow down the feasible region delimited by the three constraints, but the feasible region will always exist. Moreover, the shape of the three constraints indicates the feasible region is always convex.

SIMULATION ANALYSIS

Without the loss of generality, the following first-order process was used for the simulation throughout this paper:

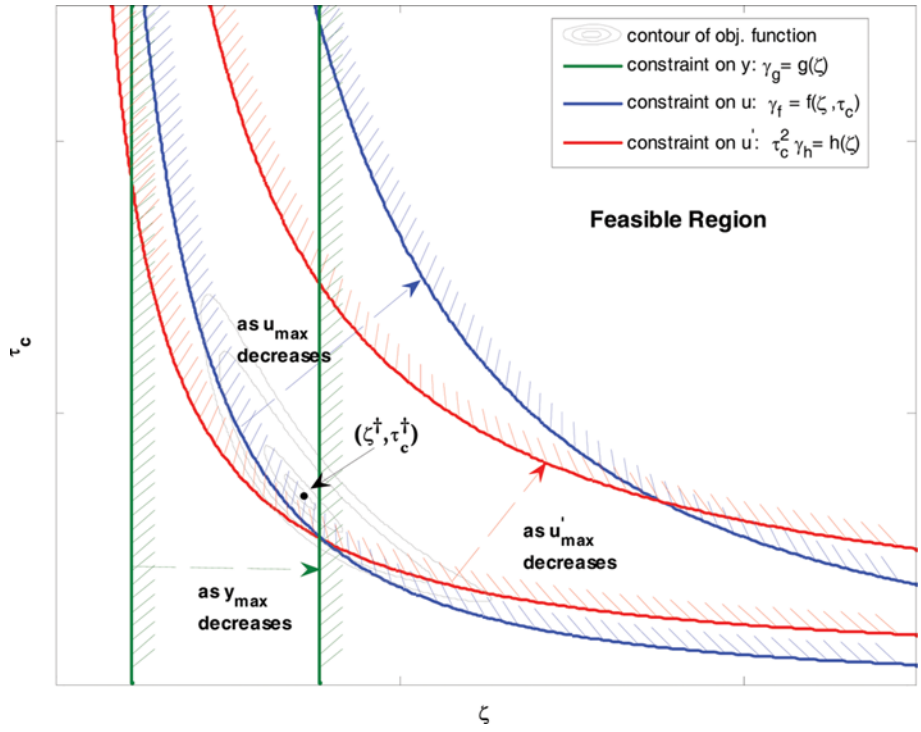

Fig. 3. Size of the feasible region as the constraints y_{max}, u_{max}, and u'_{max} decrease.

Table 2. Constraint requirements and corresponding optimal PI parameters

Example	Case	Constraint specification			PI parameter	
		y_{max}	u_{max}	u'_{max}	K_C	τ_1
1	A	1.2	0.5	1.5	1.52	1.52
2	B	1.2	0.5	0.5	0.89	1.78
3	C	1.03	0.5	1.5	1.61	1.56
4	D	1.03	0.5	1.03	1.61	1.56
5	E	1.2	0.3	1.5	1.45	2.27
6	F	1.03	0.41	1.5	1.59	1.59
7	G	1.2	0.4	1.17	2.04	1.74

$$G_p(s) = \frac{10}{10s-1} \tag{15}$$

Table 2 lists typical examples of the seven possible cases based on various constraint specifications. Simulations were carried out for weighting factors, $\omega_y = \omega_u = 0.5$; Figs. 4 and 5 present the time responses by the proposed optimal PI controller for the seven examples.

As seen in the responses, the resulting optimal PI controllers not only provide the stable and optimal closed-loop responses, but also satisfy the y_{max}, u'_{max}, and u_{max} requirements, strictly. Note that when the process model is not perfect, the responses of the system will in some cases violate the constraints and/or stability. One can compensate model uncertainties by adjusting constraint values more conservatively and also secure the stability implicitly by adjusting the weighting factors in the optimal control objective function.

DISCUSSION

In the performance index of the optimal control, the weighting factor, ω, is used to emphasize either the robustness or control performance of the system based on the designer requirements. For example, if the control objective is to have a tighter control response, the weight of the process variable, ω_y, should be increased. Similarly, a larger $\omega_{u'}$ should be chosen if the main control objective is the smoothness of the process variable rather than its speed. Fig. 6 shows the trajectories of the extreme and global optimal points in (ζ, τ_c) space as the weighting factor varies. For small values of ω_y, such as $\omega_y = 0.1$ (meaning a large value of $\omega_{u'}$), the main focus of the control system is the limitation of the controller output variable. Therefore, the optimal controller keeps the controller output and its rate of change smaller. At the same time, the proposed method ensures that the constraint specification y_{max} is not violated. This can be seen from the trajectory of the global optimum in Fig. 6. In fact, for small ω_y values, the trajectory of the global optimum follows the vertical line laid by the y_{max} constraint before shifting to the constraint laid by u'_{max} for ω_y values greater than 0.67. In addition, because the extreme point tends to be located above the constraints imposed by u_{max} and u'_{max}, the optimal control problem will fall either in case A or case C for small ω_y in Fig. 2. On the other hand, for a larger ω_y, the focus of the control system is on the limitation of the process variable. Therefore, the optimal controller keeps the process variable close to the desired set point, while satisfying the constraint imposed by the u'_{max} specification. This can be observed from Fig. 6 because the global optimum follows the constraint curve laid by the u'_{max} specification for higher values of ω_y. In addition, the extreme point

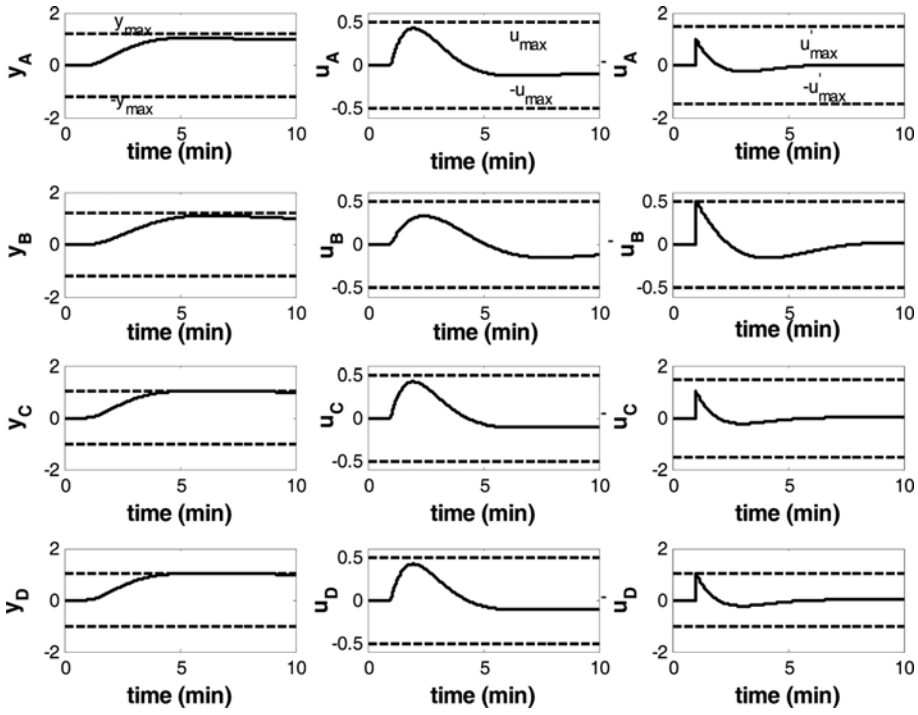

Fig. 4. Time responses of the system for cases A to D.

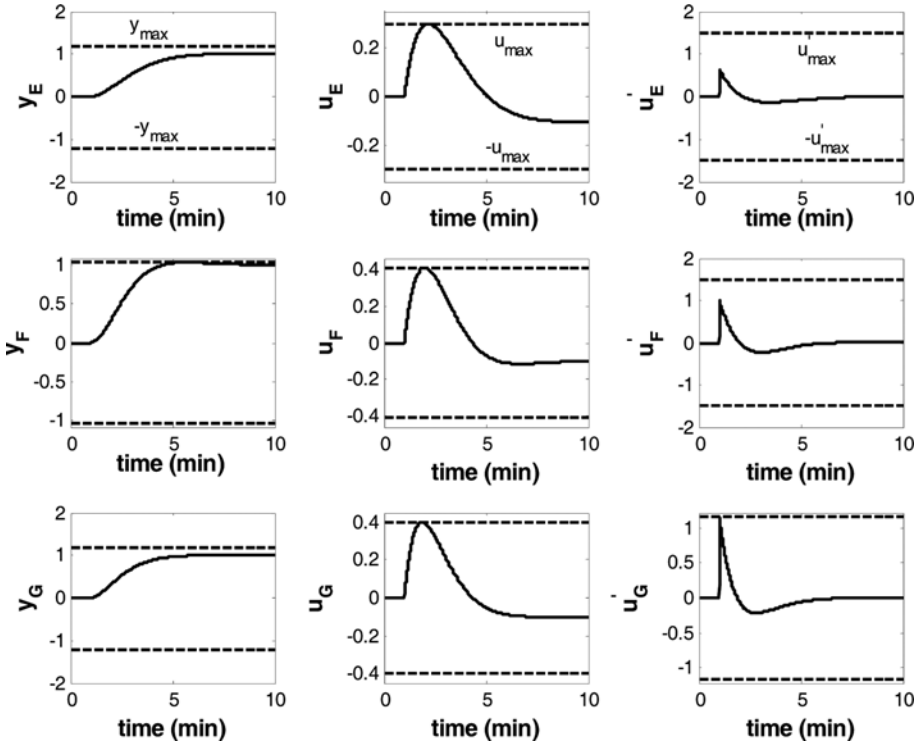

Fig. 5. Time responses of the system for Cases E to G.

shifts downward in (ζ, τ_c) space. This suggests that for higher values of ω_y, the optimal solution will probably be case B in Fig. 2.

For case A (unconstrained case), the ratio of the optimal proportional gain, K_c^{opt}, to the optimal integral time, τ_I^{opt}, is not dependent on the process parameters and is determined only by the weighting factors, ω_y and $\omega_{u'}$. Similarly, for a step input set-point, the peak value of the derivative of the control variable, u'_{peak}, is also only related to ω_y and $\omega_{u'}$ as follows:

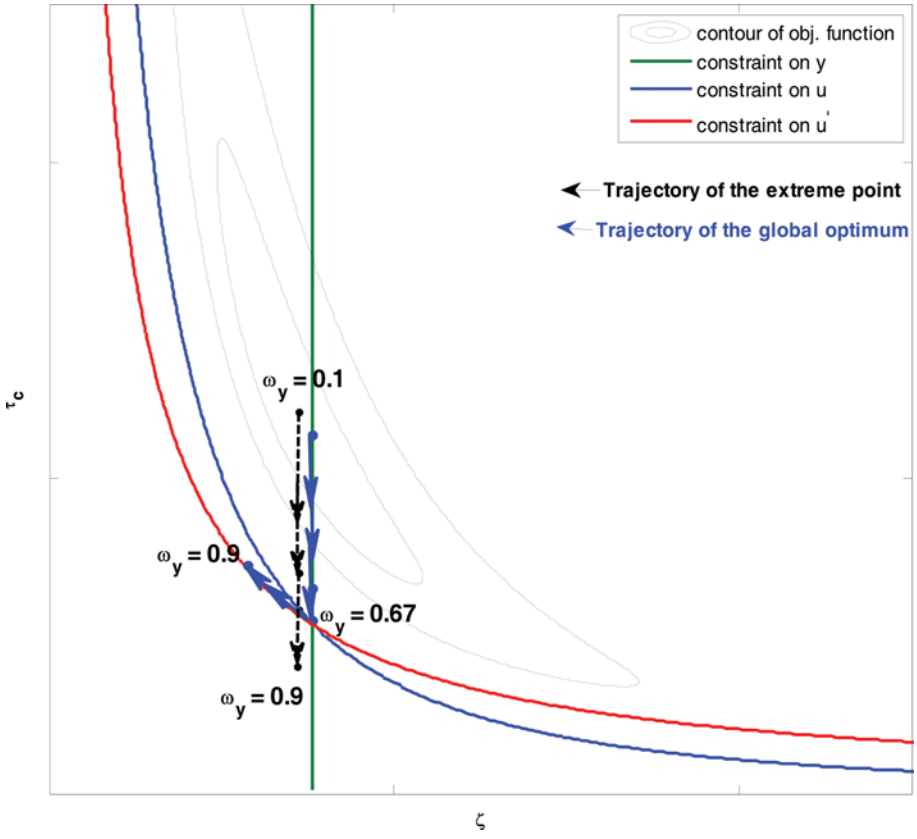

Fig. 6. Paths of the global optimum and extreme point as the weighting factor varies.

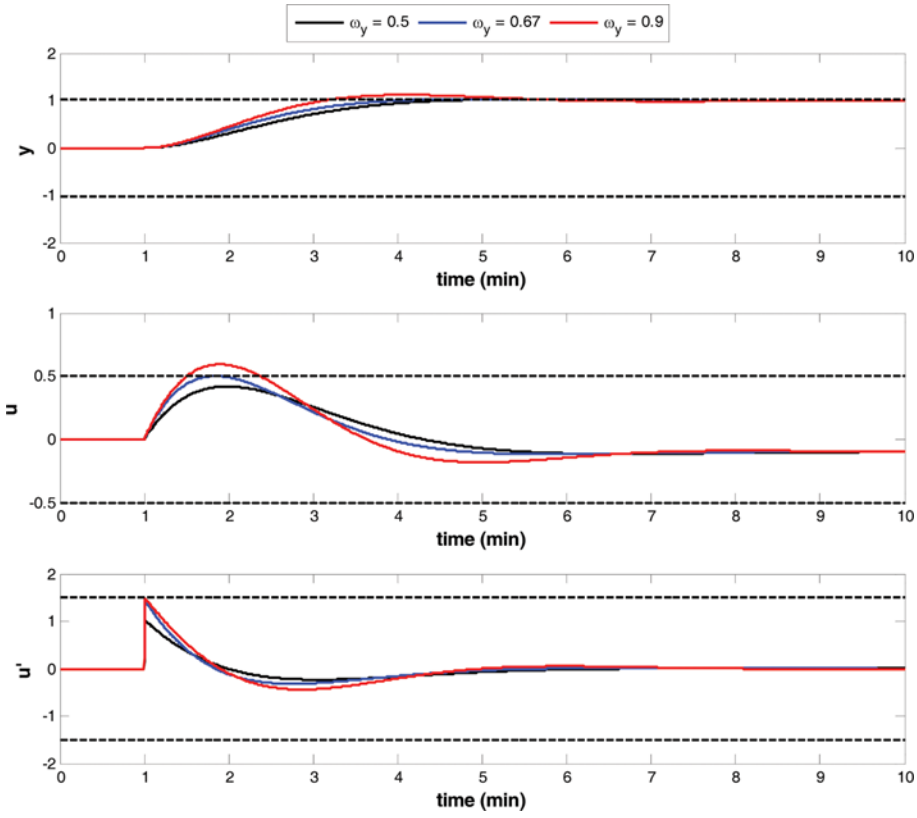

Fig. 7. Effect of the weighting factor on the responses of y (t), u (t), and u′ (t).

$$\frac{K_c^{opt}}{\tau_I^{opt}} = \frac{u'_{peak}}{\Delta Y_{sp}} = \sqrt{\frac{\omega_y}{\omega_u}} \quad (16)$$

Fig. 7 presents the corresponding closed-loop responses of the resulting PI controller for the process examined in Fig. 6 for ω_y=0.5, 0.67, and 0.9. The constraints were set arbitrarily as y_{max}=1.03, u_{max}=0.5, and u'_{max}=1.5. The inherent trade-off between the process variable and the controller output can be seen in this figure. An increase in ω_y leads to a faster and tighter control response, and conversely, a decrease in ω_y (or an increase in $\omega_{u'}$) makes the controller output and its rate smoother and smaller. For ω_y=0.5, only y_{max} constrains the optimal control response, i.e., case C. For ω_y= 0.67, the system is now constrained by u_{max} and u'_{max}, i.e., case G, as confirmed by the observation of Fig. 6. As ω_y increases to ω_y= 0.9, u'_{max} now constrains the optimal response, i.e., case B.

CONCLUSIONS

A closed-form analytical design of proportional-integral (PI) controller parameters was developed for the optimal control of an open-loop unstable first-order process subject to operational constraints. Owing to astute parameterization, a complex constrained optimal control problem can be reformulated and converted to a simple algebraic form, from which an analytical solution of the optimal control can be derived for the open-loop unstable process subject to multiple operational constraints. Graphical analysis of the constraints and objective function contour can then be performed easily in the new parameter space, through which analytical solutions of the optimal PI controller can be derived without having to rely on the numerical or black-box optimization effort. The proposed closed form solution of the constrained optimal controller establishes a direct relationship between the control and plant parameters. This provides rapid insight into how the control parameters affect the plant. Moreover, the optimal PI parameters can be obtained in an easy and quick manner, but also guarantee the global optimality of the solution. Although the proposed approach is based on a basic first-order unstable system, it can be extended to other higher dynamics unstable systems by applying model reduction techniques, a semi-analytical approach, and the IMC structure with internal stabilization techniques.

ACKNOWLEDGEMENTS

This study was supported by a Yeungnam university grant in 2016.

NOMENCLATURE

D(s) : external disturbance
e(t) : error of the process variable
K : gain of the process
K_c : proportional gain of the controller
U(s) : control variable transfer function
u(t) : control variable time function
u_{max} : maximum acceptable value of the control variable
u'_{max} : maximum acceptable value of the rate of change of the control variable
u′(t) : rate of change of the control variable time function
Y(s) : process variable transfer function
Y_{sp}(s) : set point transfer function
y(t) : process variable time function
y_{max} : maximum acceptable value of the process variable
ΔY_{sp} : maximum step change expected in the set point
ζ : damping coefficient
σ_i : slack variable
τ : time constant of the plant [min]
τ_I : integral time constant of the system [min]
ϖ_i : Lagrangian multiplier
ω_y, $\omega_{u'}$, ω : weighting factors

REFERENCES

1. J. C. Mankin and J. L. Hudson, *Chem. Eng. Sci.*, **39**, 1807 (1984).
2. K. H. Javed, T. Mahmud and E. Purba, *Chem. Eng. Res. Des.*, **84**, 465 (2006).
3. R. Zhang, A. Xue and S. Wang, *Chem. Eng. Sci.*, **66**, 6002 (2011).
4. T. Miyajima, T. Fujita, K. Sakaki, K. Kawashima and T. Kagawa, *Prec. Eng.*, **31**, 156 (2007).
5. R. Horowitz, Y. Li, K. Oldham, S. Kon and X. Huang, *Con. Eng. Prac.*, **15**, 291 (2007).
6. H. P. Huang and C. C. Chen, *J. Chem. Eng. Jpn.*, **32**, 486 (1999).
7. C. S. Jung, H. K. Song and J. C. Hyun, *J. Process Control*, **9**, 265 (1999).
8. E. F. Jacob and M. Chidambaram, *Comput. Chem. Eng.*, **20**, 579 (1996).
9. C. Edwards and I. Postlethwaite, *Automatica*, **34**, 199 (1998).
10. D. Q. Mayne, J. B. Rawlings, C. V. Rao and P. O. M. Scokaert, *Automatica*, **36**, 789 (2000).
11. M. Bak, Control of Systems with Constraints, Department of Automation, Technical University of Denmark, Denmark (2000).
12. M. Lee and J. Shin, *Chem. Eng. Commun.*, **196**, 729 (2009).
13. M. Lee, J. Shin and J. Lee, *Hydrocarbon Processing*, **89**, 71 (2010).
14. M. Lee, J. Shin and J. Lee, *Hydrocarbon Processing*, **89**, 81 (2010).
15. V. H. Nguyen, Y. Yoshiyuki and M. Lee, *J. Chem. Eng. Jpn.*, **44**, 345 (2011).
16. H. Thu and M. Lee, *Korean J. Chem. Eng.*, **30**, 2151 (2013).
17. I. B. Vapnyarskii, Springer, Heidelberg (2001).
18. S. Boyd and L. Vandenberghe, Cambridge University Press., Cambridge (2004).

APPENDICES

Appendix A. Derivation of the Performance Index of the System

The performance index of the system is defined as

$$\phi=\int_0^\infty [\omega_y(y(t)-y_\infty)^2+\omega_u(u'(t)-u'_\infty)^2]dt \tag{A1}$$

When the system is subjected to a step change in the set point of the process variable, $Y_{sp}=\Delta Y_{sp}/s$, the final values of y, u, and u′ are given as

$$y_\infty=y(\infty)=\Delta Y_{sp};\ u_\infty=u(\infty)=-\frac{\Delta Y_{sp}}{K};\ u'_\infty=u'(\infty)=0 \tag{A2}$$

Therefore, using the inverse Laplace of Eqs. (1) and (2), the following equations can be obtained:

$$\begin{aligned} e(t)&=y(t)-y_\infty=\alpha_y e^{r_1 t}+\beta_y e^{r_2 t}\\ u'(t)-u'_\infty&=\alpha_u e^{r_1 t}+\beta_u e^{r_2 t}\end{aligned} \tag{A3}$$

with

$$\alpha_y=\frac{-\beta_0\Delta Y_{sp}}{r_1};\ \beta_y=\frac{\beta_0\Delta Y_{sp}}{r_2};$$

$$\beta_0=\begin{cases}\dfrac{i}{4x\tau_c\zeta^2}=\dfrac{i}{\varepsilon x\tau_I} & \text{for } 0<\zeta\le 1\\ -\dfrac{1}{4x\tau_c\zeta^2}=-\dfrac{1}{\varepsilon x\tau_I} & \text{for } \zeta>1\end{cases} \tag{A4}$$

and

$$r_1=\frac{-1+x}{2\tau_c};\ r_2=\frac{-1-x}{2\tau_c} \tag{A5}$$

where

$$\begin{aligned} x&=i\frac{\sqrt{1-\zeta^2}}{\zeta} \quad \text{for } 0<\zeta\le 1\\ &=\frac{\sqrt{\zeta^2-1}}{\zeta} \quad \text{for } \zeta>1\end{aligned} \tag{A6}$$

The performance index can be rewritten as

$$\begin{aligned}\phi=\Bigg[&\omega_y\left(\frac{\alpha_y^2 e^{2r_1 t}}{2r_1}+\frac{2\alpha_y\beta_y e^{(r_1+r_2)t}}{r_1+r_2}+\frac{\beta_y^2 e^{2r_2 t}}{2r_2}\right)\\ &+\omega_{u'}\left(\frac{\alpha_u^2 e^{2r_1 t}}{2r_1}+\frac{2\alpha_{u'}\beta_u e^{(r_1+r_2)t}}{r_1+r_2}+\frac{\beta_u^2 e^{2r_2 t}}{2r_2}\right)\Bigg]_0^\infty.\end{aligned} \tag{A7}$$

Because r_1 and r_2 are the roots of the characteristic equation, $\varepsilon\tau_c\tau_I s^2+\varepsilon\tau_I s+1=0$, the following relationship are true:

$$\begin{aligned} r_1+r_2&=-2\omega_n\zeta=\frac{-1}{\tau_c};\\ r_1 r_2&=\omega_n^2=\frac{1}{\varepsilon\tau_c\tau_I};\ r_1-r_2=\frac{x}{\tau_c}\end{aligned} \tag{A8}$$

As we can notice, $r_1+r_2<0$; and $r_1r_2>0$. This means that the real parts of r_1 and r_2 are negative. Therefore, the integration of e^{rt} vanishes at infinity. Therefore, the performance index can be written as

$$\begin{aligned}\phi&=-\left[\omega_y\left(\frac{\alpha_y^2}{2r_1}+\frac{2\alpha_y\beta_y}{r_1+r_2}+\frac{\beta_y^2}{2r_2}\right)+\omega_u\left(\frac{\alpha_{u'}^2}{2r_1}+\frac{2\alpha_u\beta_{u'}}{r_1+r_2}+\frac{\beta_{u'}^2}{2r_2}\right)\right]\\ &=\frac{\omega_y\Delta Y_{sp}^2}{2}\tau_c(4\zeta^2+1)+\frac{\omega_{u'}\Delta Y_{sp}^2}{32K^2}\frac{(4\tau_c^2\zeta^2+\tau^2)}{\tau_c^3\zeta^4}\\ &=\alpha\tau_c(4\zeta^2+1)+\frac{\beta(4\tau_c^2\zeta^2+\tau^2)}{\tau^2\tau_c^3\zeta^4}\end{aligned} \tag{A9}$$

Appendix B. Derivation of the Constraint $\gamma_g\ge g(\zeta)$

From the inverse Laplace transform of Eq. (1), the time response of the process variable to a step change in the set point can be derived as follows:

$$y(t)=\begin{cases}\Delta Y_{sp}-\Delta Y_{sp}e^{-\frac{1}{2\tau_c}t}\left[\cos\left(\dfrac{x}{2\tau_c}t\right)+\dfrac{1}{x}\sin\left(\dfrac{x}{2\tau_c}t\right)\right]\\ \text{for } 0<\zeta<1\\ \Delta Y_{sp}-\Delta Y_{sp}e^{-\frac{1}{2\tau_c}t}\left(\dfrac{t}{2\tau_c}+1\right)\\ \text{for } \zeta=1\\ \Delta Y_{sp}-\Delta Y_{sp}e^{-\frac{1}{2\tau_c}t}\left[\cosh\left(\dfrac{x}{2\tau_c}t\right)+\dfrac{1}{x}\sinh\left(\dfrac{x}{2\tau_c}t\right)\right]\\ \text{for } \zeta>1\end{cases} \tag{A10}$$

As t approaches infinity, the steady-state value of the above process variable can be found as follows:

$$y_{ss}(t\to\infty)=\Delta Y_{sp} \tag{A11}$$

The time at which the largest peak in the process variable occurs can be obtained from the differentiation of the process variable, y(t), as follows:

$$\begin{aligned} t_{peak}&=\frac{2\tau_c\pi}{x} \text{ for } 0<\zeta<1\\ &=\infty \quad \text{for } \zeta\ge 1\end{aligned} \tag{A12}$$

Substituting the value of the peak time in the process variable, the peak value of y(t) can be obtained as follows:

$$y_{peak}=|\Delta Y_{sp}|g(\zeta) \tag{A13}$$

where

$$g(\zeta)=\begin{cases}1+e^{-\frac{\pi}{x}} & \text{for } 0<\zeta<1\\ 1 & \text{for } \zeta\ge 1\end{cases} \tag{A14}$$

Therefore, the constraint in (5-2) can be expressed as

$$g(\zeta)<\gamma_g=\left|\frac{y_{max}}{\Delta Y_{sp}}\right| \tag{A15}$$

Appendix C. Derivation of the Constraint $\gamma_f\ge f(\zeta,\ \tau_c)$

Applying the inverse Laplace transform to Eq. (2), the control variable can be obtained as follows:

$$u=\begin{cases} -\frac{\Delta Y_{sp}}{K}+\frac{\Delta Y_{sp}}{K}e^{-\frac{1}{2\tau_c}t}\left[\cosh\left(\frac{x}{2\tau_c}t\right)+\frac{2\tau_c\zeta^2+\tau}{2x\tau_c\zeta^2}\sinh\left(\frac{x}{2\tau_c}t\right)\right] \\ \text{for } \zeta>1 \\ -\frac{\Delta Y_{sp}}{K}+\frac{\Delta Y_{sp}}{K}e^{-\frac{1}{2\tau_c}t}\left(1+\frac{\tau+2\tau_c}{4\tau_c^2}t\right) \\ \text{for } \zeta=1 \\ -\frac{\Delta Y_{sp}}{K}+\frac{\Delta Y_{sp}}{K}e^{-\frac{1}{2\tau_c}t}\left[\cos\left(\frac{x}{2\tau_c}t\right)+\frac{2\tau_c\zeta^2+\tau}{2x\tau_c\zeta^2}\sin\left(\frac{x}{2\tau_c}t\right)\right] \\ \text{for } 0<\zeta<1 \end{cases} \tag{A16}$$

As t approaches infinity, the steady-state response of the above control variable can be expressed as

$$u_{ss}(t\to\infty)=-\frac{\Delta Y_{sp}}{K} \tag{A17}$$

The time at which the largest peak in the control variable occurs was obtained from the differentiation of u(t) as follows:

$$t_{upeak}=\begin{cases} \frac{2\tau_c}{x}\tan^{-1}\left(\frac{\tau x}{2\tau_c+\tau}\right) & \text{for } 0<\zeta<1 \\ \frac{2\tau\tau_c}{\tau+2\tau_c} & \text{for } \zeta=1 \\ \frac{2\tau_c}{x}\tanh^{-1}\left(\frac{\tau x}{2\tau_c+\tau}\right) & \text{for } \zeta>1 \end{cases} \tag{A18}$$

Therefore,

$$|u_{peak}|\le u_{max}\Rightarrow\left|\frac{\Delta Y_{sp}}{K}\right|f(\zeta,\tau_c)\le u_{max} \tag{A19}$$

where

$$f(\zeta,\tau_c)=\begin{cases} \left|-1+\frac{\sqrt{4\tau_c(\tau_c+\tau)\zeta^2+\tau^2}}{2\tau_c\zeta}e^{-\frac{1}{x}\tan^{-1}\left(\frac{\tau x}{2\tau_c+\tau}\right)}\right| & \text{for } 0<\zeta<1 \\ \left|-1+e^{-\frac{\tau}{\tau+2\tau_c}\left(\frac{2\tau_c+\tau}{2\tau_c}\right)}\right| & \text{for } \zeta=1 \\ \left|-1+\frac{\sqrt{4\tau_c(\tau_c+\tau)\zeta^2+\tau^2}}{2\tau_c\zeta}e^{-\frac{1}{x}\tanh^{-1}\left(\frac{\tau x}{2\tau_c+\tau}\right)}\right| & \text{for } \zeta>1 \end{cases} \tag{A20}$$

Appendix D. Derivation of the Constraint $\tau_c^2\gamma_h\ge h(\zeta)$

By differentiating the control variable, the rate of change in the control variable, u′(t), can be written as

$$u'(t)=\begin{cases} \frac{1}{4}\frac{\Delta Y_{sp}}{K\tau_c^2\zeta^2}e^{-\frac{1}{2\tau_c}t}\left[\tau\cos\left(\frac{x}{2\tau_c}t\right)-\frac{2\tau_c+\tau}{x}\sin\left(\frac{x}{2\tau_c}t\right)\right] \\ \text{for } 0<\zeta<1 \\ \frac{2\tau\tau_c-(\tau+2\tau_c)t}{8K\tau_c^3}\Delta Y_{sp}e^{-\frac{1}{2\tau_c}t} \\ \text{for } \zeta=1 \\ \frac{1}{4}\frac{\Delta Y_{sp}}{K\tau_c^2\zeta^2}e^{-\frac{1}{2\tau_c}t}\left[\tau\cosh\left(\frac{x}{2\tau_c}t\right)-\frac{2\tau_c+\tau}{x}\sinh\left(\frac{x}{2\tau_c}t\right)\right] \\ \text{for } \zeta>1 \end{cases} \tag{A21}$$

As t approaches infinity, the steady-state response of u′(t) can be expressed as

$$u'_{ss}(t\to\infty)=0 \tag{A22}$$

By setting du′(t)/dt=0, the peak of u′(t) can be found theoretically. However, the theoretical peak time obtained from this differentiation is not the actual peak time because it can be shown that, at t=0, the value, u′(0), is greater than the actual peak time. Hence, the actual peak time is u′(0)

$$\begin{aligned} &\forall\zeta>0, \\ &t_{u'tpeak}=0 \\ &|u'_{peak}|<u'_{max}\Rightarrow\left|\frac{\tau}{K}\frac{\Delta y_{sp}}{\tau_c^2}\right|h(\zeta)\le u'_{max} \end{aligned} \tag{A23}$$

where

$$h(\zeta)=\frac{1}{4\zeta^2}\quad\text{for } \zeta>0 \tag{A24}$$